ON THE ROLE OF STIFF SOIL DEPOSITS ON SEISMIC GROUND SHAKING IN WESTERN LIGURIA, ITALY: EVIDENCES FROM PAST EARTHQUAKES AND SITE RESPONSE

Roberto De Ferrari[1], Gabriele Ferretti[1], Simone Barani[1], Giacomo Pepe[1], Andrea Cevasco[1]

[1] Dipartimento di Scienze della Terra dell'Ambiente e della Vita, Università degli Studi di Genova, Corso Europa 26, 16132 Genova, Italy.

Corresponding author: Roberto De Ferrari (deferrari@dipteris.unige.it)

Published on ENGINEERING GEOLOGY, vol. 226, p. 172-183, ISSN: 0013-7952, 2017

doi: 10.1016/j.enggeo.2017.06.006

Abstract

In this work, we analyze the macroseismic fields of the main historical earthquakes occurred in western Liguria (northwestern Italy) in order to identify possible relations between the isoseismal patterns and the local geological setting. Anomalies in the spatial distribution of macroseismic intensities are often attributed to site effects. We observed that, in the region of study, such anomalies are mainly located in areas characterized by outcropping Pliocene soil deposits, mainly made up of stiff silty and marly clays. To investigate the influence of such deposits on ground response, both horizontal-to-vertical spectral ratio measurements and numerical site response analyses were carried out. For all sites analyzed, the spectral ratio curves show marked amplification peaks between 2 and 5 Hz. Following such empirical evidence, equivalent linear ground response analyses were performed in order to examine the relation between the measured resonance frequencies and the response of a set of soil columns presenting Pliocene marly-clayey deposits at their top. To this end, a database of geotechnical and geophysical properties, including more than 50 reference soil profiles, was compiled. This database was used to define alternative numerical models considering three different ranges of thickness of the Pliocene marly-clayey deposits (between 5 and 35 m, 30 and 65 m, 60 and 105 m). Results show marked amplification effects in the ranges 1-3 Hz, 2-5 Hz, and 3-10 Hz depending on the thickness of the investigated soil deposits. These frequency ranges are in agreement with those observed from the experimental measurements, which are therefore proved adequately representative of the resonance frequencies of the Pliocene marly-clayey deposits. Therefore, based on our findings, such deposits can be considered an essential factor in producing the "anomalies" observed in the isoseismal patterns of the macroseismic fields of the historical earthquakes occurred in western Liguria.

Keywords: ground motion amplification, HVSR, site effects, ground response, damage pattern.

1. Introduction

The distribution of the total economic and human losses produced by a strong earthquake may be related to both seismological and engineering factors. While the former are inherent to the earthquake characteristics, such as source properties (e.g., rupture process, fault geometry) and seismic wave propagation between the source and the earth surface, the latter depend on the structural features and the asset exposure. Near-surface geological conditions represent the link between these factors. On the one hand, geology may affect the seismic motion by modifying its frequency content, amplitude, and duration. On the other hand, the modifications to the ground motion caused by local geology may affect the dynamic behaviours of the buildings exposed to the seismic shaking and, consequently, the total losses produced by an earthquake. The effects of local geology, which can be incorporated into probabilistic seismic hazard analyses (e.g., Bazzurro and Cornell, 2004; Rodriguez-Marek et al., 2014; Barani et al., 2014; Barani and Spallarossa, 2016; Barani et al., 2016), are commonly termed as site effects. In areas characterized by complex geomorphology and/or particular soil conditions (e.g., sites characterized by soft soils overlying rock formations), the definition of site effects represents one of the most important issues of seismology and earthquake engineering (e.g., Massa et al., 2004; Gallipoli et al., 2004; Parolai et al., 2010; De Ferrari et al., 2010; Edwards et al., 2013; Massa et al., 2014; Massa et al., 2016; Mascandola et al., 2017). Site effects can be examined either through experimental methods or by using numerical approaches. Experimental methods consist of computing spectral ratios of earthquake recordings relative to a reference site (Borcherdt, 1970) or to the vertical component of the same recording at a single station (Lermo and Chávez-Garcia, 1993). When horizontal-to-vertical spectral ratios (HVSRs) are based on ambient noise recordings, the technique is known as Nakamura's method (Nakamura, 1989). Numerical approaches simulate the dynamic behavior of soils and, depending on the local geomorphological features to be modeled, can be distinguished into mono- or multi-dimensional methods (Kramer, 1996).

The application of site response methods may be guided by the knowledge of local geology or by the analysis of the damage distribution produced by past earthquakes, which is often influenced by site effects. For instance, De Ferrari et al. (2010) applied both experimental and numerical methods (1D and 2D) in order to corroborate the hypothesis of ground shaking amplification deduced by the analysis of the macroseismic field of the 1920 Garfagnana earthquake (moment magnitude M_w = 6.5). D'Amico et al. (2002) validated the same anomalies through HVSR measurements.

This study was prompted by observation of "anomalies" (i.e., sites with intensities of at least one degree greater than surroundings) in the macroseismic fields of the strongest historical earthquakes occurred in western Liguria (e.g., 1564 earthquake with M_w = 5.8, 1831 earthquake with M_w = 5.6, 1854 earthquake with M_w = 5.7, 1887 earthquake with M_w = 6.3, 1963 earthquake with M_w = 6.0 (Locati et al., 2016)) and the knowledge of the regional distribution of Pliocene deposits, thus suggesting a possible relationship between them. In light of this evidence, this study investigates the role of some Pliocene deposits, which mainly consist of stiff marly clays, on seismic amplification through the application of experimental and numerical site response methods. Amplification effects related to stiff soil deposits, such as those just mentioned, are poorly documented in literature. Only few authors focused on this issue starting from the observation of irregular damage patterns (e.g., Bouckovalas and Kouretzis, 2001; Lekkas, 2001). Furthermore, since current anti-seismic codes give special emphasis to soft soils, the role of stiff soils or weak rocks on ground motion amplification may be overlooked. In western Liguria, many towns and settlements are built on Pliocene marly-clayey deposits. Moreover, some of the populated areas are characterized by high density of inhabitants enhancing the seismic risk. It is therefore evident the importance of investigating the seismic behaviour of such materials in order to outline future seismic risk mitigation strategies.

This paper first presents a brief overview of the historical seismicity of western Liguria, examining correlations between the geographic distribution of macroseismic anomalies and that of Pliocene stiff marly-clayey deposits. Subsequently, geotechnical data and spectral ratio measurements are

described. Results of such measurements are then compared with the response of a set of typical stratigraphic settings of Pliocene clayey soils, which is evaluated through 1D numerical ground response analyses.The goal of our study is twofold. On the one hand, it allows attaining a better knowledge of the seismic behavior of the Pliocene stiff marly-clayey deposits. On the other one, it allows verifying their influence on the anomalies observed in the macroseismic fields of historical earthquakes occurred in the study region.

2. Data and methods

2.1. Evidences of macroseismic anomalies

Western Liguria is one of the seismically most active regions in northwestern Italy (e.g., Barani et al., 2010). It is characterized by moderate to strong seismicity, both distributed in well defined onshore areas and along the main active faults in the Ligurian Sea (e.g., Barani et al., 2007; Scafidi et al., 2015). As observed above, large earthquakes have occurred in the past, the largest one with magnitude 6.3 on February 23, 1887 at 5:21 a.m. (UTC time). Analyzing the distribution of the felt intensities produced by this earthquake (Locati et al., 2016), the largest damage and losses were concentrated in municipalities where Pliocene deposits outcrop (Figure 1). For instance, the intensity value associated with Diano Castello (purple circle in Figure 1) is equal to X MCS (Mercalli-Cancani-Sieberg), which results two-to-three degrees greater than the one associated with the surrounding municipalities like Varcavello and Diano San Pietro, where the intensities reached VII and VIII MCS, respectively (see Figure 1). Similar anomalies are observed for Bussana Vecchia (IX), Pompeiana (VIII-IX), and Vallecrosia (VIII): at these sites, the observed intensities are one-to-two degrees greater than those associated with the surrounding municipalities. Macroseismic anomalies also emerge from the macroseismic fields relative to other significant earthquakes occurred in western Liguria. For instance, the macroseismic fields of the 1831 (M_w= 5.6) and 1854 (M_w = 5.7) earthquakes (see at http://emidius.mi.ingv.it/CPTI15-DBMI15/) again show intensities

that, at the site of Bussana (VIII MCS and VII-VIII MCS, respectively), are generally greater, by about one-to-two degrees, than those observed in the surroundings (between VI and VII MCS). In addition, also the site of Castellaro, which is located about one kilometer west of Pompeiana, presents an intensity that is unexpectedly higher compared to those associated with the surrounding sites in the macroseismic field of the 1831 earthquake. At this site the CEDIT catalogue (Martino et al., 2014) reports a slope failure induced by this earthquake.

Interestingly, the macroseimic anomalies observed at the previous sites correlate well with the geographical distribution of the Pliocene stiff clayey soils. This is interpreted as a hint of site effects, which will be discussed in the following.

2.2. Geologic framework

In the Liguria region, Pliocene deposits only crop out along the western coast between the city of Genova and the Italy-France border (Figure 1). Since the second half of the last century, these Pliocene sediments have been exhaustively studied by a great deal of researchers in order to understand their stratigraphic, sedimentological, paleontological, and structural features (Capponi et al., 2008; Giammarino et al., 2010). The Liguria Pliocene deposits are considered a post-orogenic sedimentary cover. They are usually trapped in East-West or North-South trending fault-controlled basins, which are interpreted as grabens. These tectonic structures are related to the Plio-Quaternary tectonic up-lift, which involved a large part of the Ligurian coast after the main phases of both Alpine and North Apennine orogens. Therefore, tectonic events played a key role in controlling the evolution of the Liguria Pliocene sedimentation. These extensional tectonic events led to a continental margin morphology characterized by structurally controlled lows (grabens) filled by sediments and highs (horsts) affected by rapid dismantling. Such structural evolution is also clearly recognizable in the continental shelf of the Ligurian Sea.

The Pliocene succession has a maximum thickness of about 450 m (Marini, 2001) and unconformably overlies a substratum characterized by different rocks. Along the western and

eastern coastal sectors of the considered area, the bedrock generally consists of Cretaceous to Eocene turbidite complexes (Pepe et al., 2015). Conversely, along the stretch comprised between the towns of Genova and Savona, the Pliocene deposits overlay the metamorphic belt of the Ligurian Alps (metaophiolites, meta-acidic volcanics, and metasediments) (Crispini and Capponi, 2001; Carobene and Cevasco, 2011).

The Liguria Pliocene deposits are currently grouped into two lithostratigraphic formations (bottom to top): the Argille di Ortovero Fm. and the Conglomerati di Monte Villa Fm.. The former consists of compact deep marine marly clays (up to 150m thick) with siltstone and fine sandstone bodies interbedded. The latter (with maximum thicknesses of about 300 m) groups a number of deep sea fan-delta coarse-grained clastic deposits. Based on paleontological content, the Pliocene deposits generally date back to the Lower Pliocene. However, sedimentary bodies attributable to the Upper Pliocene-Lower Pleistocene are also reported. The Argille di Ortovero Fm. is widely spread over all the considered study area. Conversely, fan-delta bodies only crop out in the westernmost sector.

2.3. Geotechnical classification

Based on results of laboratory tests (i.e., grain size analyses, Atterberg limits, and physical determinations) collected from technical reports of civil engineering projects, the investigated materials were classified according to the Unified Soil Classification System (USCS). Figure 2a summarizes the grain-size composition of 63 soil samples. In general, the majority of the soil samples (94%) can be classified as silty and clayey soils while the remaining ones (6%) as silty sandy soils. Silty and clayey soils mainly include silt with low plasticity (ML) and clay with low (CL) and high plasticity (CH). Moreover, this category of soil shows fine content that ranges between 51.3 and 99.8%, a sandy component ranging from 0.2 to 45.4%, and a gravelly fraction ranging from 0 to 31.3%. Silty sandy soils predominantly consist of silty sand (SM) and clayey sand (SC) characterized by fine content lower than 50%, sandy component up to 50.8%, and a gravelly fraction up to 21%.

Based on Casagrande's plasticity chart (Figure 2b), the fine-grained fraction can be classified as clay with low plasticity (CL) for about 70% of the total samples. About 17% can be classified as clay with high plasticity (CH), whereas the remaining 13% as silt characterized by low plasticity (ML). Although it is somewhat variable, the content of calcium carbonate $CaCO_3$ is on overage lower than 30% (Giammarino et al., 2010).

Table 1 and frequency histograms in Figure 3 summarize the main geotechnical properties of the Argille di Ortovero Fm. The plasticity index (*PI*), which was derived from samples within 30 m depth, is somewhat variable, ranging between 3.2% and 43.4%. The total unit weight (γ) ranges from 16.8 to 21.7 kN/m^3 over a depth range of about 70 m. Finally, the values of shear wave velocity (V_S), which were gathered from technical reports of downhole measurements, seismic refraction surveys, and multichannel analysis of surface waves, are comprised between 400 m/s and 700 m/s and correspond to maximum small-strain shear modulus (G_{max}) values of about 1000 MPa (Table 1 and Figure 3). It is noteworthy that both the maximum values of V_S and G_{max} are compatible with those of soft rocks, confirming that the examined soil materials are characterized by high stiffness. This is also in agreement with the results collected from 10 incremental loading oedometer tests carried out on undisturbed specimens sampled at depth lower than 30 m. These tests revealed that these soils are mechanically overconsolidated with maximum over-consolidation ratio (OCR) values sometimes greater than 15.

2.4. Site response analysis

2.4.1. Experimental measurements

Forty-five HVSR measurements of approximately 40 minutes were carried out using Lennartz LE-3D/5s seismometers connected to MarsLite dataloggers. All measurements were performed at sites where Pliocene deposits outcrop. Each ambient noise recording was divided into windows of 40s and the respective Fourier spectra relative to both the horizontal (NS and EW) and vertical (Z) components were smoothed by applying the Konno and Ohmachi (1998) function. Finally, mean

H/V ratios and their standard deviation were computed. As an example, Figure 4 shows the H/V curves obtained for different case studies corresponding to sites located on outcropping Pliocene deposits (see Figure 1). Further H/V ratios will be presented in the final discussion where a possible application of our results is presented (see Figure 12, to come). As is clear from this figure, experimental data show marked amplification peaks, which altogether span the range 1-10Hz. Such behavior is common to the other measurement sites.

2.4.2. Numerical modeling

Based on the empirical evidences of site effects described in the previous section, 1D ground response analyses were carried out using Shake91 (Idriss and Sun, 1992) with the aim of verifying whether the results from the experimental measurements are actually in agreement with the response of the Pliocene lithotypes. To this end, a set of ten real accelerograms recorded on rock outcrop (i.e., $V_{S,30}$ > 800 m/s), consistent with the regional seismic hazard (for medium-to-long mean return periods, 475 < MRP < 2475 years) and the relevant disaggregation scenarios, was first selected and then driven at the base of different soil columns. As shown in Barani et al. (2009), the PGA and 0.2 s-spectral acceleration hazard for an MRP of 475 years in the study area is controlled by small-to-moderate magnitude events (4.5 < M < 5.5) at variable distance, R. This latter tends to increase moving from the westernmost sector of the study region, where it is within 20 km, towards the center, where it can be up to 80 km. At longer spectral periods (up to 2 s), the dominating magnitude increases of an amount of about 0.5 unit, reaching up values of about 6.5 moving towards central Liguria. R varies between 10 and 20 km in the westernmost sector, reaching up to 120 km near Savona. Increasing the MRP, M tends to increase while R decreases. The accelerograms were selected from a large data set of time histories, collecting both weak and strong ground motions, by using the procedure described in Barani et al. (2008). Selection was done in order to match as close as possible the worst case scenario in the study area (i.e., the Uniform Hazard Spectrum, UHS, for an MRP of 475 years presenting the highest spectral acceleration values). No ground motion scaling or modification is applied in this study. The main characteristics

of the selected accelerograms are summarized in Table 2. Figure 5 shows the 5%-damped acceleration response spectra of the selected records. The selected accelerograms are properly applied as outcrop motion at the base of each numerical model. This is necessary to correct for the effect of free surface.

In order to define 1D soil models representative of local stratigraphic settings, a database of geotechnical and geophysical properties, including 54 soil profiles, was compiled. Data derived from boreholes, downhole measurements, seismic refraction profiles, multichannel analysis of surface waves, and HVSRs were used to constrain both the geotechnical (e.g., shear wave velocity, total unit weight, shear strength modulus, and plasticity index) and the geometrical properties of the soil models. Most of such data refer to sites where the macroseismic anomalies have been observed. The geotechnical properties of the Pliocene marly-clayey deposits were already presented in Table 1 and Figure 3. In addition, Figure 6 shows the frequency distributions of the bedrock characteristics, including V_S, γ, and bedrock depth (h). This latter parameter is equivalent to the thickness of the Pliocene clays, which ranges between 5 m and 110 m. V_S varies between approximately 900 and 1400 m/s, whereas γ is in the range 24-28 kN/m^3.

The selection of the shear modulus reduction (G/G_{max}) and damping (D) curves for the numerical simulations was driven by *PI*. It is widely recognized that *PI* plays an important role on the dynamic behavior of soils (e.g., Vucetic and Dobry, 1991; Ishibashi and Zhang, 1993). The effect of soil plasticity is modelled here using the curves proposed by Vucetic and Dobry (1991). According to the data available (see Figure 3, top panel), the curves proposed for *PI* = 15% are adopted down to 30 m depth while those corresponding to *PI* = 50% are used for deeper, stiffer soils.

Since most Pliocene marly-clayey deposits in the study area directly overlay the bedrock and present no significant variations along the same profile, simple numerical models including two or three layers were considered appropriate for a generic characterization of the response of such materials. Given the scope of work, the high frequency contribution of shallow thin soil deposits has been neglected. The purpose of the 1D analysis is simply to verify the consistency of the

experimental observations in terms of resonance frequencies. In the numerical simulations, the Pliocene deposits were subdivided into different groups as a function of thickness. Specifically, we examined three representative stratigraphic scenarios: thin deposits ($5 < h < 35$ m), medium-thickness deposits ($30 < h < 65$ m), and thick deposits ($60 < h < 105$ m). In the first case, the Pliocene deposits were modeled has a single layer overlying the bedrock. In the remaining scenarios, they are subdivided into two separate layers that differ only by the modulus reduction and damping curves according to the variation of *PI* at depth. Besides the uncertainty in the soil thickness, we took into account the uncertainty in the shear wave velocity, total unit weight, modulus reduction and damping curves of each soil layer. To this end, 2000 Monte Carlo simulations were carried out for each target soil column following the procedure outlined by Barani et al. (2013). The main scope of the randomization was to represent most of the stratigraphic settings characterized by the Pliocene formation in western Liguria. Figure 7 shows the variability of V_S and γ along each one of the three stratigraphic scenarios considered.

As stated above, numerical ground response analyses were performed using Shake91, which implements an equivalent linear approach to model the non-linear response of soils. As a result of the numerical simulations, the amplification function, $AF(f)$, (defined as the modulus of the corresponding transfer function), the resonance frequency, f_0, and a frequency-independent amplification factor, F_a, were obtained for each soil model. According to the Eurocode 8 (Comité Européen de Normalisation – CEN, 2004), F_a is defined as the ratio of the acceleration spectrum intensity (Von Thun et al. 1988) at the surface (ASI^S) to the acceleration spectrum intensity at the rock outcrop (ASI^R) (e.g., Pergalani et al., 1999; Rey et al., 2002; Barani and Spallarossa, 2016):

$$F_a = \frac{ASI^S}{ASI^R} \quad (1)$$

The acceleration spectrum intensity is calculated as follows:

$$ASI = \int_{0.05}^{2.5} S_a(T)dT \quad (2)$$

where $S_a(T)$ indicates the 5%-damped spectral acceleration at the oscillator period T.

3. Results

Figure 8 summarizes the results of all HVSR measurements. Precisely, it shows the frequency distribution of the fundamental frequency f_0 as obtained from whole set of ambient noise measurements. In most cases, f_0 lies in the frequency range 1-3 Hz while fewer measurements indicate resonances between 3 and 6 Hz, and between 6 and 9 Hz. Most thick deposits present fundamental frequencies less than 2 Hz, medium-thickness deposits lie in the f_0 range 2-4 Hz, while thin Pliocene covers show f_0 above 4 Hz.

Similarly, Figure 9 shows the results of the numerical modeling through histograms displaying the distribution of f_0 for the three stratigraphic scenarios considered. The values of f_0 derive from the numerical amplification functions shown in the left panel of the same figure. Analogous distributions for F_a are displayed in Figure 10 along with the 5%-damped acceleration response spectra resulting from the ground response analysis. As shown in Figure 9, the fundamental frequency of the Pliocene deposits depends on the depth of the bedrock. f_0 lies between 1 and 3 Hz in the case of thick deposits, between 2 and 5 Hz for medium-thickness Pliocene soils, and is scattered above 3 Hz in the case of thin deposits. Such frequency ranges are in agreement with the ones derived from the experimental measurements (Figure 8). Therefore, they can be considered adequately representative of the resonance frequencies of the Pliocene deposits.

As is evident from Figure 10, the seismic amplification effects due to the Pliocene marly-clayey deposits is anything but negligible. The amplification factors are greater than 1.2 (such value is proposed by the Eurocode 8 for sites with $V_{S,30}$ comprised between 360 and 800 m/s in regions where the major contribution to the hazard derives from M5.5+ earthquakes) for all scenarios incorporating thick and medium-thickness Pliocene deposits, and for 62% of the models relative to thin deposits. F_a is greater than 1.35 (which is proposed by the Eurocode 8 for sites with $V_{S,30}$ comprised between 360 and 800 m/s in areas where the major contribution to the hazard derives

from earthquakes of magnitude up to 5.5) for 83%, 76%, and 23% of the scenarios corresponding to thick, medium-thickness, and thin Pliocene deposits, respectively.

Figure 11 relates the level of soil amplification, quantified by F_a, with both the thickness (h) (top panel) of the Pliocene deposits and with their fundamental period (T_0) (bottom panel) as resulted from the numerical analyses. This figure clearly shows an increasing amplification for thicknesses up to about 30 m and fundamental periods lower than 0.2 s. For greater thicknesses and T_0 values, F_a can be assumed almost stable.

4. Discussion

In this study, seismic amplification effects were indirectly deduced from the analysis of the geographic distributions of the macroseismic intensities associated with the strongest historical earthquakes in western Liguria. We observed that larger intensities are associated with sites located on outcropping Pliocene stiff soils, mainly made up of silty and marly clays of the Argille di Ortovero Fm. The seismic response of such deposits was investigated through experimental (i.e., HVSR measurements) and numerical analyses for different stratigraphic scenarios, pointing out the large influence of such materials on site amplification in many areas of western Liguria.

Since in western Liguria many urban areas are located over Pliocene stiff soils, our findings are of clear interest to local authorities and the civil engineering community to outline future seismic risk mitigation strategies. In this regard, results of our study can be used for zonation purposes. As an example, Figure 12 presents a zonation map for the Municipality of Castellaro, showing the spatial distribution of the Pliocene deposits with the associated amplification factor ranges as derived from Figures 10 and 11. Three zones, presenting Pliocene deposits of different thickness, are identified based on the fundamental frequencies obtained from the HVSR measurements (according to the ranges displayed in Figure 8).

In literature, other studies have pointed out the impact of stiff deposits on ground shaking amplification. Examining patterns of damage distribution due to the Athens (Greece) earthquake

(M_S=5.9) occurred on September 7, 1999, Bouckovalas and Kouretzis (2001) show that stiff soils, consisting of slightly moderate cemented conglomerates and clayey marl, amplified the peak horizontal acceleration by more than 40%. Based on seismic response studies performed for the city of Benevento (Italy) using seismological and geological data, Di Giulio et al. (2008) found that the weak velocity contrast between some Pliocene stiff clays (with V_S of around 600-800 m/s) and the underlying bedrock could be responsible for moderate amplification at low frequency. After the earthquake that struck L'Aquila (Italy) on April 6, 2009 (e.g., Barani and Eva, 2011), Lanzo and Pagliaroli (2012) found evidences of ground motion amplification caused by stiff soils (in that case, alluvium deposits). More recently, amplification effects due to clayey materials have been reported by Vella et al. (2013), even though these soils appear less stiff than those considered in this research (V_S lower than 500 m/s) and are characterized by different states of compaction/fracturing. A further example is presented in Hailemikael et al. (2016), where the authors examine the relative contribution of stiff covers and irregular topography on the ground motion amplification at the Colle di Roio ridge, L'Aquila (Central Italy).

In light of the previous observations, the role of stiff soils would deserve major attention in anti-seismic provisions for design. We found that soil amplification factors associated with geological settings characterized by outcropping Pliocene stiff marly-clayey deposits overlying a harder bedrock often exceed the values of 1.2 and 1.35 proposed by the Eurocode 8 for sites presenting dense/stiff materials with $V_{S,30}$ comprised between 360 and 800 m/s and thickness of several tens of meters. According to Dobry and Iai (2000), such finding points out possible limitations of anti-seismic norms that use $V_{S,30}$ as a proxy to seismic amplification in areas characterized by deep, stiff soils lying on much harder rock. In such conditions and, more generally, in case of complex or particular geological scenarios, defining the seismic action for design can be a critical issue. These phenomena are widely debated in the literature, pointing out the importance of refined site classifications based on proxies superseding the limitations of $V_{S,30}$ (e.g., Barani et al., 2008;

Castellaro et al., 2008; Gallipoli and Mucciarelli, 2009; Luzi et al., 2011; Di Alessandro et al., 2012; Pitilakis et al., 2013).

5. Conclusions

The findings of this research have shown that the presence of stiff clayey soils is determinant for site amplification in western Liguria. Pronounced amplification peaks are observed in the following frequency ranges: 1-3, 3-10, and 2-5 Hz corresponding to soil thickness intervals of 60-105, 30-65, and 5-35 m, respectively. Such findings are in agreement with the outcomes of 1D numerical analyses performed for different scenarios representative of the seismic response of the Pliocene soils. Such an agreement indicates that experimental observations are actually representative of the resonance frequencies of the Pliocene marly-clayey soils in this region. This confirms that the anomalies observed in the macroseismic fields of past western Liguria earthquakes are mainly attributable to the presence of such subsurface materials. In addition, also irregular topography and seismically induced slope failures may have contributed to the damage produced by past earthquakes at some localities where the investigated deposits outcrop at the crest of relatively steep slopes. Future research could refine the analysis of site effects presented here, examining the relative contribution of topography and stratigraphy to the total amplification. Nevertheless, this study provides a valuable contribution to the definition and refinement of seismic risk mitigation strategies and urban planning.

Acknowledgements

We are thankful to the Editor and to the two anonymous reviewers for their thorough review and helpful suggestions, which brought improvements to the article.

References

Ambraseys, N., Smit, P., Sigbjornsson, R., Suhadolc, P., Margaris, B., 2002, Internet-site of European strong motion data. European Commission, Research-Dictorate General, Environment and Climate Programme.

Ancheta, T. D., Darragh, R. B., Stewart, J. P., Seyhan, E., Silva, W., Chiou, B., Wooddell, K. E., Graves, R. W., Kottke, A. R., Boore, D. M., et al., 2014, NGA-West2 database, Earthq. Spectra 30, 989-1005. DOI:10.1193/070913EQS197M

Barani, S., De Ferrari, R., Ferretti, G., Eva, C., 2008. Assessing the effectiveness of soil parameters for ground response characterization and soil classification. Earthq. Spectra 24(3), 565–597. DOI:10.1193/1.2946440

Barani, S., Eva, C., 2011. Did the 6 April, 2009 L'Aquila earthquake fill a seismic gap? Seismol. Res. Lett. 82, 645-653. DOI:10.1785/gssrl.82.5.645

Barani, S., Spallarossa, D., Bazzurro, P., 2009. Disaggregation of probabilistic ground-motion hazard in Italy. Bull. Seismol. Soc. Am. 99, 2638-2661. DOI:10.1785/0120080348

Barani, S., Scafidi, D., Eva, C., 2010. Strain rates in Northwestern Italy from spatially smoothed seismicity. J. Geophys. Res. 115, B07302. DOI:10.1029/2009JB006637

Barani, S., De Ferrari, R., Ferretti, G., 2013. Influence of soil modeling uncertainties on site response. Earthq. Spectra 29(3), 705-732. DOI:10.1193/1.4000159

Barani, S., Massa, M., Lovati, S., Spallarossa, D., 2014. Effects of surface topography on ground shaking prediction: implications for seismic hazard analysis and recommendations for seismic design. Geophys. J. Int. 197, 1551-1565. DOI:10.1093/gji/ggu095

Barani, S., Albarello, D., Spallarossa, D., Massa, M., 2016. Empirical scoring of ground motion prediction equations for probabilistic seismic hazard analysis in Italy including site effects. Bull. Earthq. Eng. DOI:10.1007/s10518-016-0040-3.

Barani, S., Spallarossa D., 2016. Soil amplification in probabilistic ground motion hazard analysis. Bull. Earthq. Eng. DOI:10.1007/s10518-016-9971-y.

Barani, S., Spallarossa D., Bazzurro P., Eva, C., 2007, Sensitivity analysis of seismic hazard for Western Liguria (North Western Italy): A first attempt towards the understanding and quantification of hazard uncertainty. Tectonophysics 435, 13-35. DOI:10.1016/j.tecto.2007.02.008

Bazzurro, P., Cornell, C.A., 2004. Nonlinear soil-site effects in probabilistic seismic-hazard analysis. Bull. Seismol. Soc. Am. 94, 2110-2123.

Bouckovalas, G.D., Kouretzis, G.P., 2001. Stiff soil amplification effects in the 7 September 1999 Athens (Greece) earthquake. Soil Dyn. Earthq. Eng. 21, 671-687. DOI:10.1016/S0267-7261(01)00045-8

Capponi, G., Crispini, L., Bonci, M.C., Cabella, R., Cavallo, C., Cortesogno, L., Fabbri, B., Federico, L., Firpo, M., Gaggero, L., Nosengo, S., Ottonello, G., Piazza, M., Perilli, N., Piccazzo, M., Ramella, A., Spagnolo, C., Vannucci, G., Vetuschi Zuccolini, M., 2008. Note Illustrative della Carta Geologica d'Italia alla scala 1:50.000 - Foglio "Genova" n. 213-230. Apat e Regione Liguria, S.EL.CA., Firenze.

Carobene, L., Cevasco, A., 2011. A large scale lateral spreading, its genesis and Quaternary evolution in the coastal sector between Cogoleto and Varazze (Liguria - Italy). Geomorphology, 129(3), 398-411. DOI:10.1016/j.geomorph.2011.03.006

Castellaro, S., Mulargia, F., Rossi, P.L., 2008. VS30: Proxy for seismic amplification? Seismol. Res. Lett. 79, 540-543. DOI:10.1785/gssrl.79.4.540

Comité Européen de Normalisation (CEN), 2004. prENV 1998-1-Eurocode 8: Design of structures for earthquake resistance. Part 1: General rules, seismic actions and rules for buildings, Draft No. 4, Brussels, Belgium.

Crispini, L., Capponi, G., 2001. Tectonic evolution of the Voltri Group and Sestri Voltaggio Zone (southern limit of the NW Alps): a review. Ofioliti 26, 161–164.

D'Amico, V., Albarello, D., Mucciarelli, M., 2002. Validation through HVSR measurements of a method for the quick detection of site amplification effects from intensity data: an application to a

seismic area in Northern Italy. Soil Dyn. Earthq. Eng. 22, 475-83. DOI:10.1016/S0267-7261(02)00031-3

De Ferrari, R., Ferretti, G., Barani, S., Spallarossa, D., 2010. Investigating on the 1920 Garfagnana earthquake (Mw=6.5): Evidences of site effects in Villa Collemandina (Tuscany, Italy). Soil Dyn. Earthq. Eng. 30, 1417-1429. DOI:10.1016/j.soildyn.2010.07.004

Di Alessandro, C., Bonilla, L.F., Boore, D.M., Rovelli, A., Scotti, O., 2012. Predominant-period site classification for response spectra prediction equations in Italy Bull. Seismol. Soc. Am. 102(2), 680-695. DOI:10.1785/0120110084

Di Giulio, G., Improta, L., Calderoni, G., Rovelli, A., 2008. A study of the seismic response of the city of Benevento (southern Italy) through a combined analysis of seismological and geological data. Eng. Geol. 97, 146-170. DOI:10.1016/j.enggeo.2007.12.010

Dobry, R., Iai, S., 2000. Recent developments in the understanding of earthquake site response and associated seismic code implementation. Proceedings of GeoEng2000. An International Conference on Geotechnical & Geological Engineering, Melbourne, Australia, pp 186–219.

Edwards, B., Michel, C., Poggi, V., Fäh, D., 2013. Determination of site amplification from regional seismicity. Seismol. Res. Lett. 84, 611-621. DOI:10.1785/0220120176

Gallipoli, M.R., Mucciarelli, M., Gallicchio, S., Tropeano, M., Lizza, C., 2004. HVSR measurements in the area damaged by the 2002 Molise, Italy earthquake. Earthq. Spectra 20, 81-94. DOI:10.1193/1.1766306

Gallipoli, M.R., Mucciarelli, M., 2009. Comparison of site classification from VS30, VS10, and HVSR in Italy. Bull. Seismol. Soc. Am. 99, 340-351. DOI:10.1785/0120080083

Giammarino, S., Fanucci, F., Orezzi, S., Rosti, D., Morelli, D., Cobianchi, M., De Stefanis, A., Di Stefano, A., Finocchiaro, F., Fravega, P., Piazza, M., Vannucci, G., 2010. Note Illustrative della Carta Geologica d'Italia alla scala 1:50.000 - Foglio "San Remo" n.258-271. ISPRA - Regione Liguria. A.T.I. - SystemCart s.r.l. - L.A.C. s.r.l. - S.EL.CA., Firenze.

Hailemikael, S., Lenti, L., Martino, S., Paciello, A., Rossi, D., Mugnozza, G.S., 2016. Ground-motion amplification at the Colle di Roio ridge, central Italy: a combined effect of stratigraphy and topography. Geophys. J. Int. 206(1), 1-18. DOI:10.1093/gji/ggw120

Idriss, I.M., Sun, J.I., 1992. User's manual for Shake91: A computer program for conducting equivalent linear seismic response analyses of horizontally layered soil deposits, Center for Geotechnical Modeling, Department of Civil and Environmental Engineering, University of California, Davis.

Ishibashi, I., Zhang, X., 1993. Unified dynamic shear moduli and damping ratios of sand and clay. Soils Found. 33, 182-191.

Konno, K., Ohmachi, T., 1998. Ground motion characteristics estimated from spectral ratio between horizontal and vertical components of microtremor. Bull. Seismol. Soc. Am. 88, 228-241.

Kramer, S.L., 1996. Geotechnical earthquake engineering. Prentice-Hall, New Jersey.

Lanzo, G., Pagliaroli, A., 2012. Seismic site effects at near-fault strong-motion stations along the Aterno River Valley during the Mw=6.3 2009 L'Aquila earthquake. Soil Dyn. Earthq. Eng. 40, 1-14. DOI:10.1016/j.soildyn.2012.04.004

Lekkas, E., 2001. The Athens earthquake (7 September 1999): intensity distribution and controlling factors. Eng. Geol. 59, 297-311. DOI:10.1016/S0013-7952(00)00119-8

Lermo, J., Chavez-Garcia, F.J., 1993. Site effect evaluation using spectral ratios with only one station. Bull. Seismol. Soc. Am. 83, 1574-1594.

Locati, M., Camassi, R., Rovida, A., Ercolani, E., Bernardini, F., Castelli, V., Caracciolo, C.H., Tertulliani, A., Rossi, A., Azzaro, R., D'Amico, S., Conte, S., Rocchetti, E., 2016. DBMI15, the 2015 version of the Italian Macroseismic Database. Istituto Nazionale di Geofisica e Vulcanologia. DOI:10.6092/INGV.IT-DBMI15

Luzi, L., Hailemikael, S., Bindi, D., Pacor, F., Mele, F., Sabetta, F., 2008. ITACA (ITalian ACcelerometric Archive): a web portal for the dissemination of Italian strong-motion data. Seismol. Res. Lett. 79, 716-722. DOI:10.1785/gssrl.79.5.716

Luzi, L., Puglia, R., Pacor, F., Gallipoli, M.R., Bindi, D., Mucciarelli, M., 2011. Proposal for a soil classification based on parameters alternative or complementary to Vs,30. Bull. Earthq. Eng. 9(6), 1877-1898. DOI:10.1007/s10518-011-9274-2

Marini, M., 2001. Il Pliocene Ligure fra Ventimiglia e Bordighera (Imperia, Alpi Marittime liguri); osservazioni preliminari. Boll. Soc. Geol. It. 120, 37-46.

Martino, S., Prestininzi, A., Romeo, R.W., 2014. Earthquake-induced ground failures in Italy from a reviewed database. Nat. Hazards Earth Syst. Sci. 14(4), 799-814. DOI:10.5194/nhess-14-799-2014

Mascandola, C., Massa, M., Barani, S., Lovati S., Santulin, M., 2017, Long-period amplification in deep alluvial basins and consequences for site-specific probabilistic seismic hazard analysis: an example from the Po Plain (northern Italy), Bull. Seism. Soc. Am. 107(2), 770-786. DOI:10.1785/0120160166

Massa, M., Ferretti, G., Cevasco, A., Isella, L., Eva, C., 2004. Analysis of site amplification phenomena: an application in Ripabottoni for the 2002 Molise, Italy, earthquake. Earthq. Spectra 20, 107-118. DOI:10.1193/1.1768540

Massa, M., Barani, S., Lovati, S., 2014. Overview of topographic effects based on experimental observations: meaning, causes and possible interpretations. Geophys. J. Int. 197, 1537-1550. DOI:10.1093/gji/ggt341

Massa, M., Mascandola, C., Ladina, C., Lovati, S., Barani, S., 2016. Fieldwork on local-site seismic response in the Po Plain: examples from ambient vibration array and single station analyses. Bull. Earthq. Eng. DOI:10.1007/s10518-016-0017-2

Nakamura, Y., 1989. A method for dynamic characteristics estimations of subsurface using microtremors on the ground surface. Q. Rep. RTRI Japan 30, 25-33.

Parolai, S., Orunbaev, S., Bindi, D., Strollo, A., Usupaev, S., Picozzi, M., Di Giacomo, D., Augliera, P., D'Alema, E., Milkereit, C., Moldobekov, B., Zschau, J., 2010. Site Effects Assessment in Bishkek (Kyrgyzstan) Using Earthquake and Noise Recording Data. Bull. Seismol. Soc. Am. 100(6), 3068-3082. DOI:10.1785/0120100044

Pepe, G., Piazza, M., Cevasco, A., 2015. Geomechanical characterization of a highly heterogeneous flysch rock mass by means of the GSI method. Bull. Eng. Geol. Environ. 74(2), 465-477. DOI:10.1007/s10064-014-0642-4

Pergalani, F., Romeo, R., Luzi, L., Petrini, V., Pugliese, A., Sanò, T., 1999. Seismic microzoning of the area struck by Umbria–Marche (Central Italy) Ms 5.9 earthquake of 26 September 1997. Soil Dyn. Earthq. Eng. 19, 279-296. DOI:10.1016/S0267-7261(99)00003-2

Pitilakis, K., Riga, E., Anastasiadis, A., 2013. New code site classification, amplification factors and normalized response spectra based on a worldwide ground-motion database. Bull. Earthq. Eng. 11, 925-966. DOI:10.1007/s10518-013-9429-4

Rey, J., Faccioli, E., Bommer, J.J., 2002. Derivation of design soil coefficients (S) and response spectral shapes for Eurocode 8 using the European strong-motion database. J. Seismol. 6, 547-555. DOI:10.1023/A:1021169715992

Rodriguez-Marek, A., Rathje, E.M., Bommer, J.J., Scherbaum, F., Stafford, P.J., 2014. Application of single-station sigma and site-response characterization in a probabilistic seismic-hazard analysis for a new nuclear site. Bull. Seismol. Soc. Am. 104, 1601-1619. DOI:10.1785/0120130196

Scafidi, D., Barani, S., De Ferrari, R., Ferretti, G., Pasta, M., Pavan, M., Spallarossa, D., Turino, C., 2015. Seismicity of northwestern Italy during the last thirty years. J. Seismol. 19, 201-218. DOI:10.1007/s10950-014-9461-0

Stucchi, M., Meletti, C., Montaldo, V., Crowley, H., Calvi, G.M., Boschi, E., 2011. Seismic hazard assessment (2003-2009) for the Italian building code. Bull. Seismol. Soc. Am. 101, 1885-1911. DOI:10.1785/0120100130

Vella, A., Galea, P., D'Amico, S., 2013. Site frequency response characterisation of the Maltese islands based on ambient noise H/V ratios. Eng. Geol. 163, 89-100. DOI:10.1016/j.enggeo.2013.06.006

Von Thun, J.L., Rochim, L.H., Scott, G.A., Wilson, J.A., 1988. Earthquake ground motions for design and analysis of dams, in Earthquake Engineering and Soil Dynamics II – Recent Advance in Ground motion Evaluation, Geotechnical Special Publication 20, ASCEE, New York, 463-481.

Vucetic, M., Dobry, R., 1991. Effect of soil plasticity on cyclic response. J. Geotech. Eng. 117, 89-107.

Captions

Table 1 - Geotechnical properties of the Argille di Ortovero Fm. (γ total unit weight, W_L Atterberg liquid limit, W_P Atterberg plastic limit, *PI* Plasticity Index, V_S shear wave velocity, G_{max} maximum small-strain shear modulus, CV Coefficient of Variation).

Table 2 - List of ground motion time histories used in the numerical simulations. M_w is for moment magnitude, *R* for epicentral distance, and PHA indicates peak horizontal acceleration. ESD: European Strong Motion Database (Ambraseys et al., 2002); ITACA: ITalian ACcelerometric Archive (Luzi et al., 2008); PEER: Pacific Earthquake Engineering Research ground motion database (Ancheta et al., 2014).

Figure 1 - Distribution of Pliocene deposit outcrops in Liguria (light blue areas). The macroseismic field of the 1887 earthquake (Locati et al., 2016) is superimposed in the bottom panel.

Figure 2 - Grain-size composition (a) and Casagrande's plasticity chart (b) of the Pliocene deposits. CL, CH: clays with low and high plasticity, respectively; ML, MH: silts with low and high plasticity, respectively; OL, OH: organic soils with low and high plasticity, respectively.

Figure 3 - Variability of the geotechnical properties associated with the Pliocene deposits: plasticity index (*PI*), total unit weight (γ), and shear wave velocity (V_S).

Figure 4 - Experimental H/V curves obtained at representative test sites on outcropping Pliocene deposits (the thick line indicates the mean H/V curve while the dotted lines delimit the one standard deviation error band). Stratigraphic columns are shown for each site.

Figure 5 - Linear 5%-damped acceleration response spectra (horizontal component) of the records selected for the numerical analyses. The average response spectrum and the reference 475-year uniform hazard spectrum (Stucchi et al., 2011) used in the accelerogram selection are also shown for comparison.

Figure 6 - Variability of bedrock characteristics: bedrock depth (*h*), total unit weight (γ), and shear wave velocity (V_S).

Figure 7 - Two thousand γ and *V*s profiles generated via Monte Carlo simulation for thin (left panel), medium-thickness (middle panel), and thick (right panel) Pliocene deposits (grey lines).

Figure 8 - Distribution of f_0 as obtained from the HVSR measurements.

Figure 9 - Amplification functions obtained from numerical modeling (left panels) and distributions of f_0 (right panels) for thin, medium-thickness, and thick Pliocene deposits. Each amplification function corresponds to a realization of the Monte Carlo simulation used to account for the uncertainty in the soil models.

Figure 10 - 5%-damped acceleration response spectra obtained from numerical modeling (left panels) and distributions of F_a (right panels) for thin, medium-thickness, and thick Pliocene deposits.

Figure 11 - Distribution of F_a as a function of the thickness (top panel) and fundamental period (bottom panel) of the Pliocene deposits.

Figure 12 - Zonation map of the Castellaro Municipality. The Digital Elevation Model (DEM) is shown in background (contour line interval is 25 m). Example HVSR curves are superimposed.

Table 1

	γ (kN/m^3)	W_L (%)	W_P (%)	PI (%)	V_S (m/s)	G_{max} (MPa)
Mean	19.2	40	22.8	18.0	554	589
Min	16.8	27	15.7	3.2	405	276
Max	21.7	64	31.9	43.4	700	1063
CV (%)	4.7	19	13.6	42.8	14.4	32.1

Table 2

Earthquake Name	Country	Date	Latitude	Longitude	M_w	R (km)	Station Code	PHA (g)	Databank
Bingol	Turkey	01/05/2003	39.01	40.51	6.3	14.0	BIN	0.298	ESD
Northridge	California	17/01/1994	34.21	-118.55	6.7	25.4	141	0.289	PEER
L'Aquila	Italy	07/04/2009	42.38	13.38	4.6	0.7	AQP	0.170	ITACA
Morgan Hill	California	24/04/1984	37.31	-121.70	6.2	38.6	G01	0.069	PEER
Matese	Italy	29/12/2013	41.37	14.45	5.2	23.3	BSSO	0.010	ITACA
Kocaeli, Turkey	Turkey	17/08/1999	40.73	29.99	7.5	5.3	IZT	0.220	PEER
Northridge	California	17/01/1994	34.21	-118.55	6.7	49.9	L04	0.084	PEER
San Fernando	California	09/02/1971	34.44	-118.41	6.6	24.2	L04	0.153	PEER
Northridge	California	17/01/1994	34.21	-118.55	6.7	45.8	MTW	0.234	PEER
Chi-Chi	Taiwan	22/09/1999	23.81	121.08	6.2	100.4	TCU	0.064	PEER

Figure 1

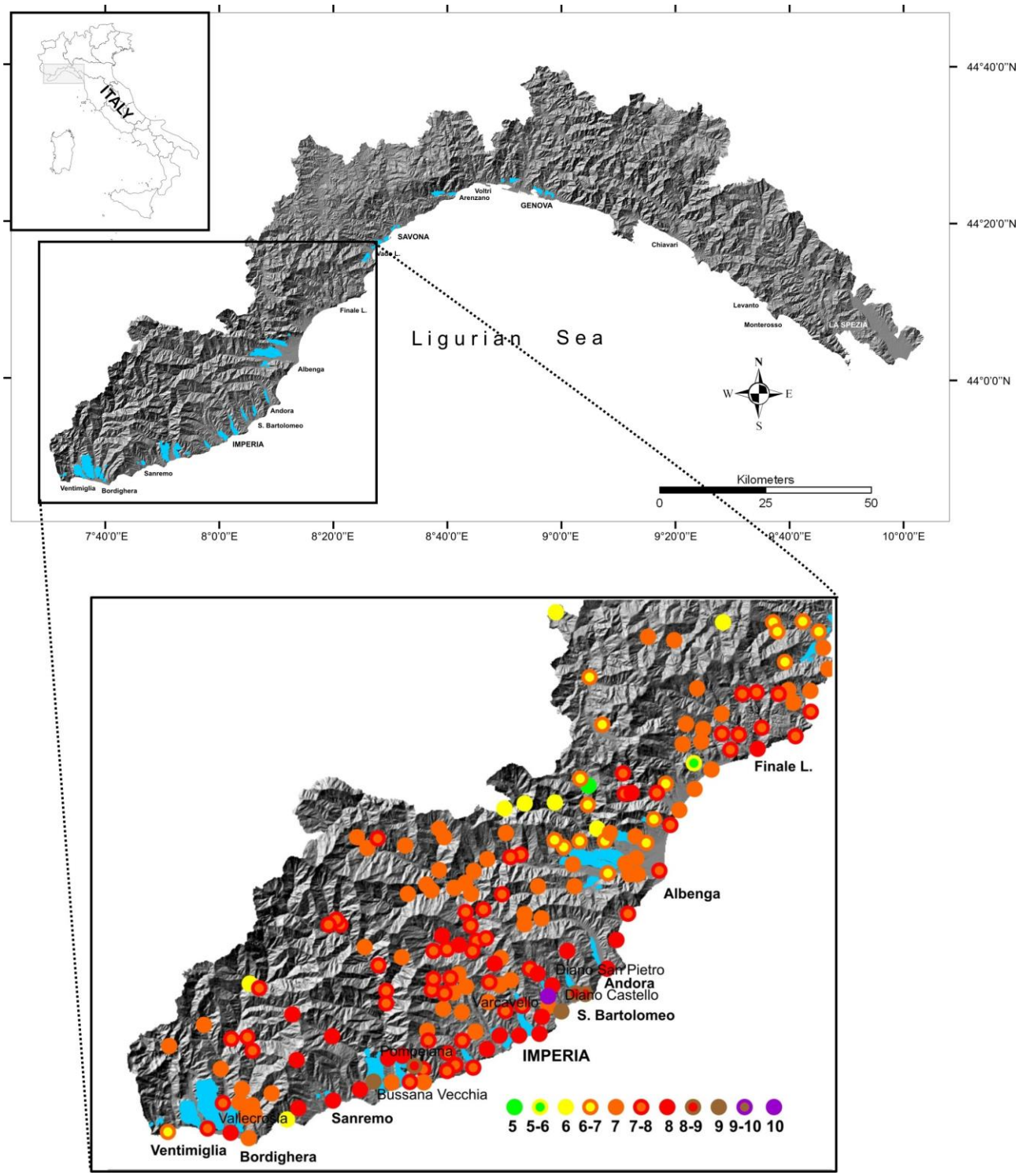
ITALY
Voltri
Arenzano
GENOVA
SAVONA
Chiavari
Levanto
Monterosso
LA SPEZIA
Finale L.
Albenga
Andora
S. Bartolomeo
IMPERIA
Sanremo
Ventimiglia
Bordighera
Ligurian Sea
N
W
E
S
Kilometers
0
25
50
44°40'0"N
44°20'0"N
44°0'0"N
7°40'0"E
8°0'0"E
8°20'0"E
8°40'0"E
9°0'0"E
9°20'0"E
9°40'0"E
10°0'0"E
Finale L.
Albenga
Diano San Pietro
Andora
Diano Castello
Varcavello
S. Bartolomeo
Pompeiana
IMPERIA
Bussana Vecchia
Vallecrosia
Sanremo
Ventimiglia
Bordighera
5 5-6 6 6-7 7 7-8 8 8-9 9 9-10 10

Figure 2

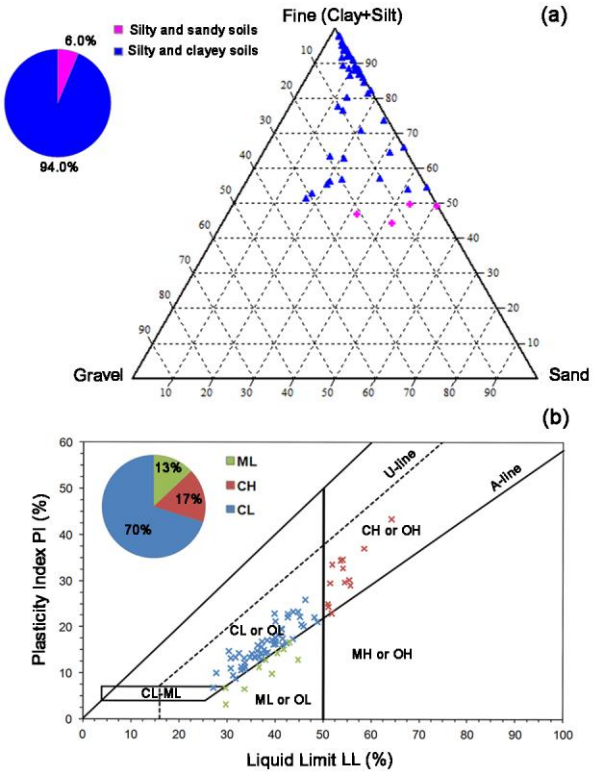
(a)
Fine (Clay+Silt)
Gravel
Sand
6.0%
94.0%
Silty and sandy soils
Silty and clayey soils
(b)
Plasticity Index PI (%)
Liquid Limit LL (%)
13%
17%
70%
ML
CH
CL
U-line
A-line
CH or OH
CL or OL
MH or OH
CL-ML
ML or OL

Figure 3

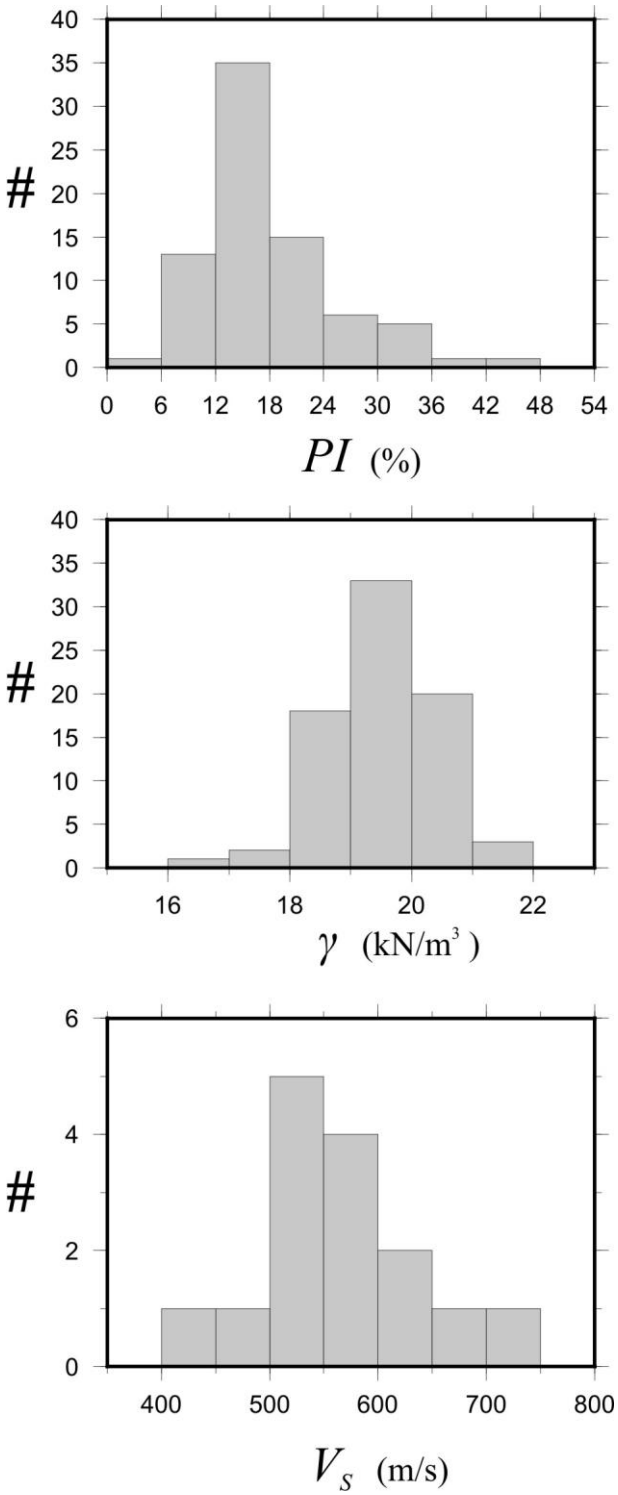

Figure 4

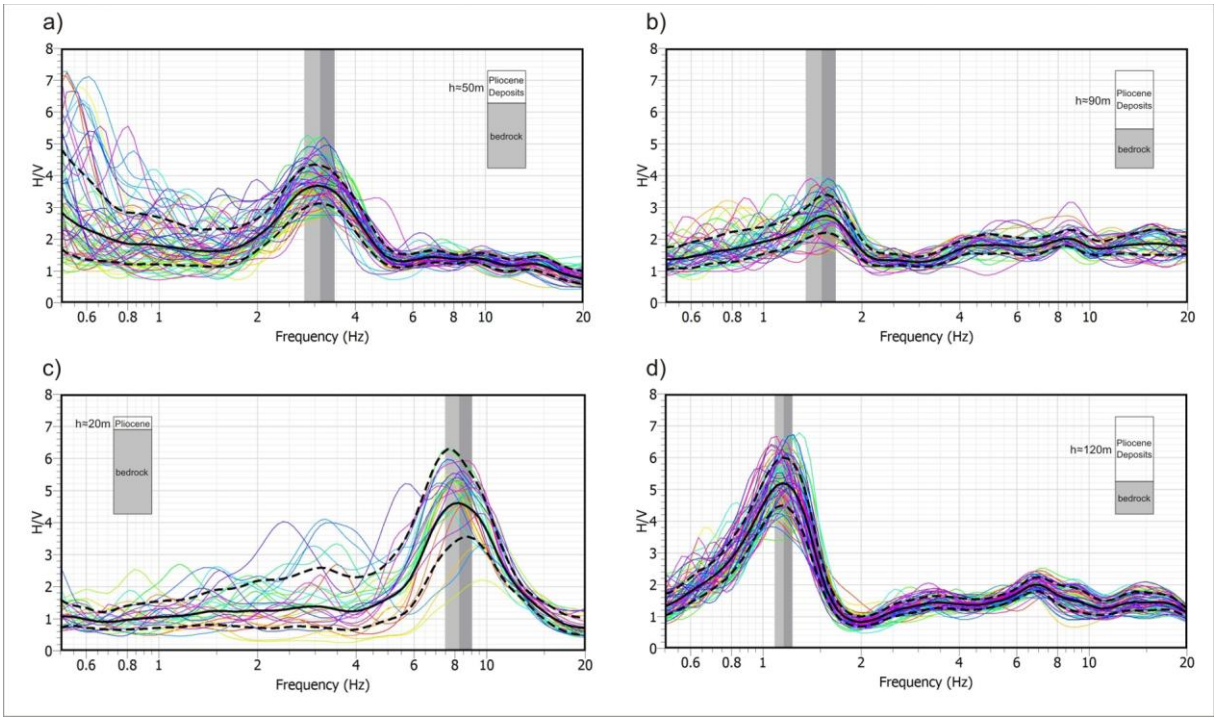
a)
h≈50m
Pliocene Deposits
bedrock
H/V
Frequency (Hz)
b)
h≈90m
Pliocene Deposits
bedrock
H/V
Frequency (Hz)
c)
h≈20m
Pliocene
bedrock
H/V
Frequency (Hz)
d)
h≈120m
Pliocene Deposits
bedrock
H/V
Frequency (Hz)

Figure 5

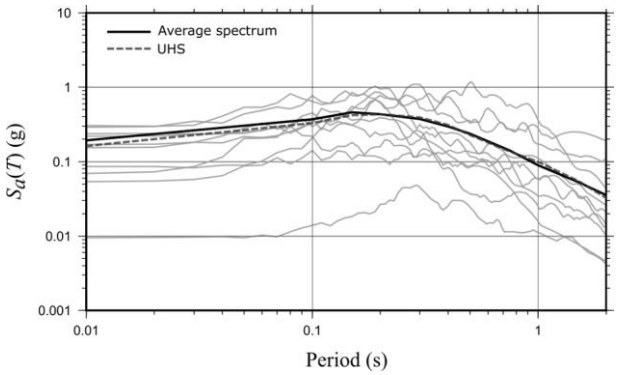

Figure 6

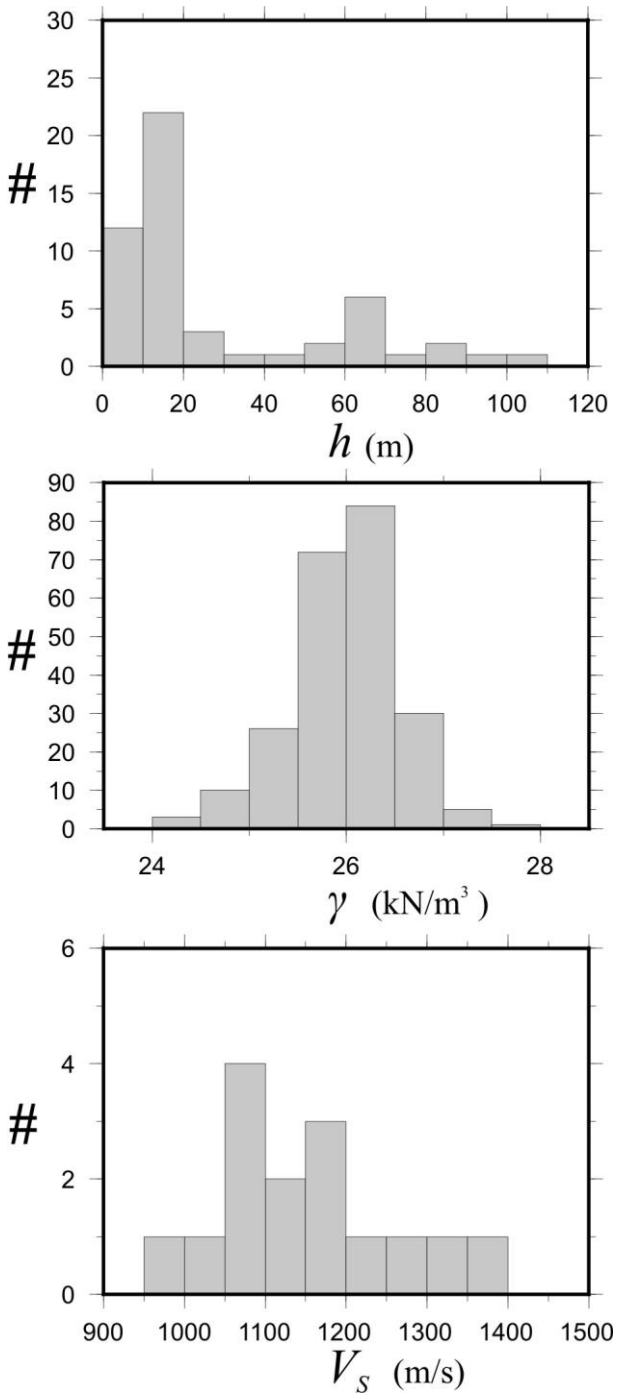

Figure 7

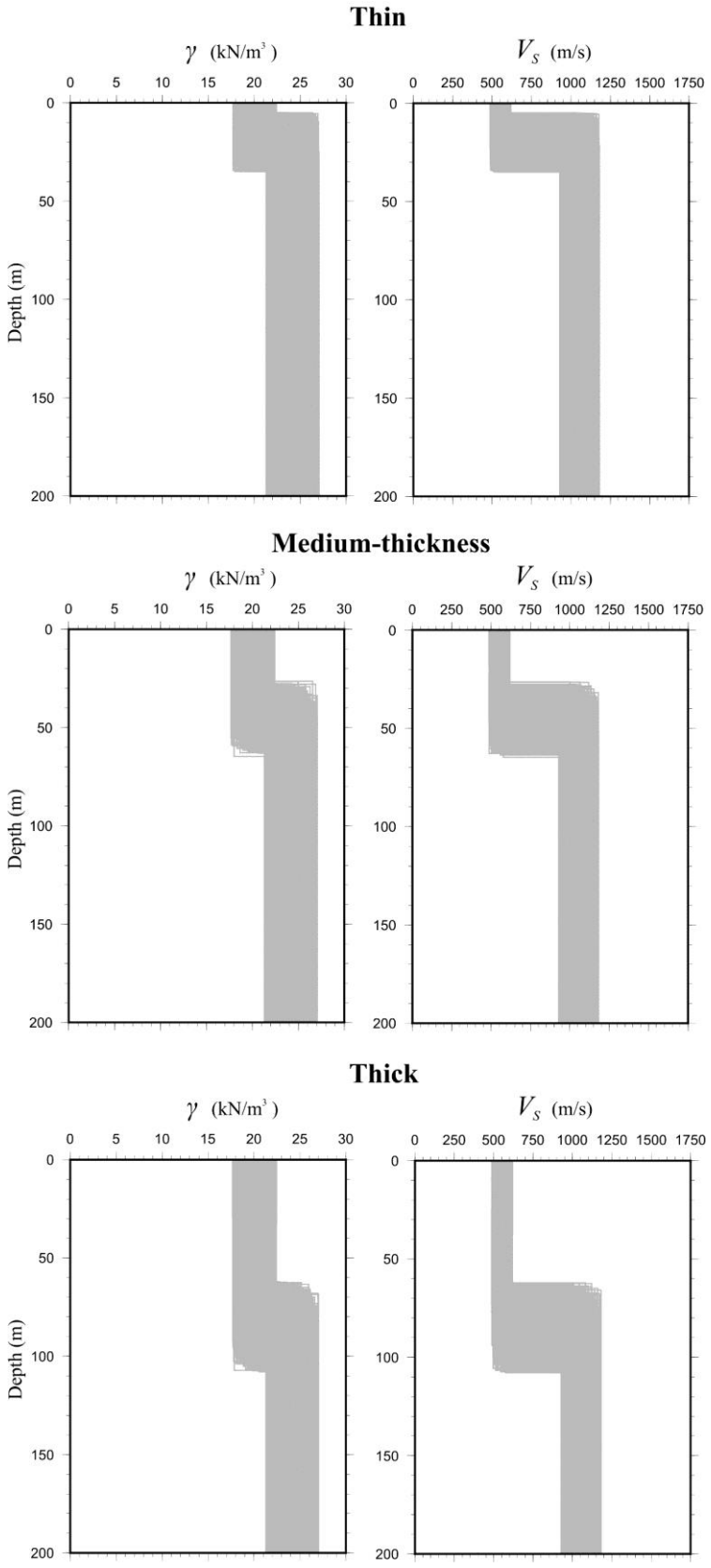
Thin
γ (kN/m³)
0 5 10 15 20 25 30
V_S (m/s)
0 250 500 750 1000 1250 1500 1750
Depth (m)
0 50 100 150 200
Medium-thickness
γ (kN/m³)
0 5 10 15 20 25 30
V_S (m/s)
0 250 500 750 1000 1250 1500 1750
Depth (m)
0 50 100 150 200
Thick
γ (kN/m³)
0 5 10 15 20 25 30
V_S (m/s)
0 250 500 750 1000 1250 1500 1750
Depth (m)
0 50 100 150 200

Figure 8

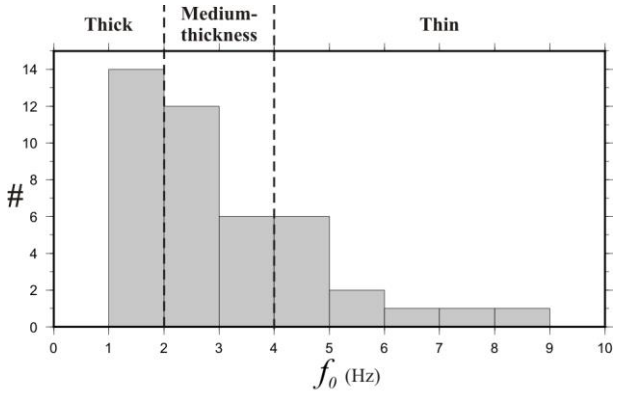
Thick
Medium-thickness
Thin
#
14
12
10
8
6
4
2
0
0
1
2
3
4
5
6
7
8
9
10
f_0 (Hz)

Figure 9

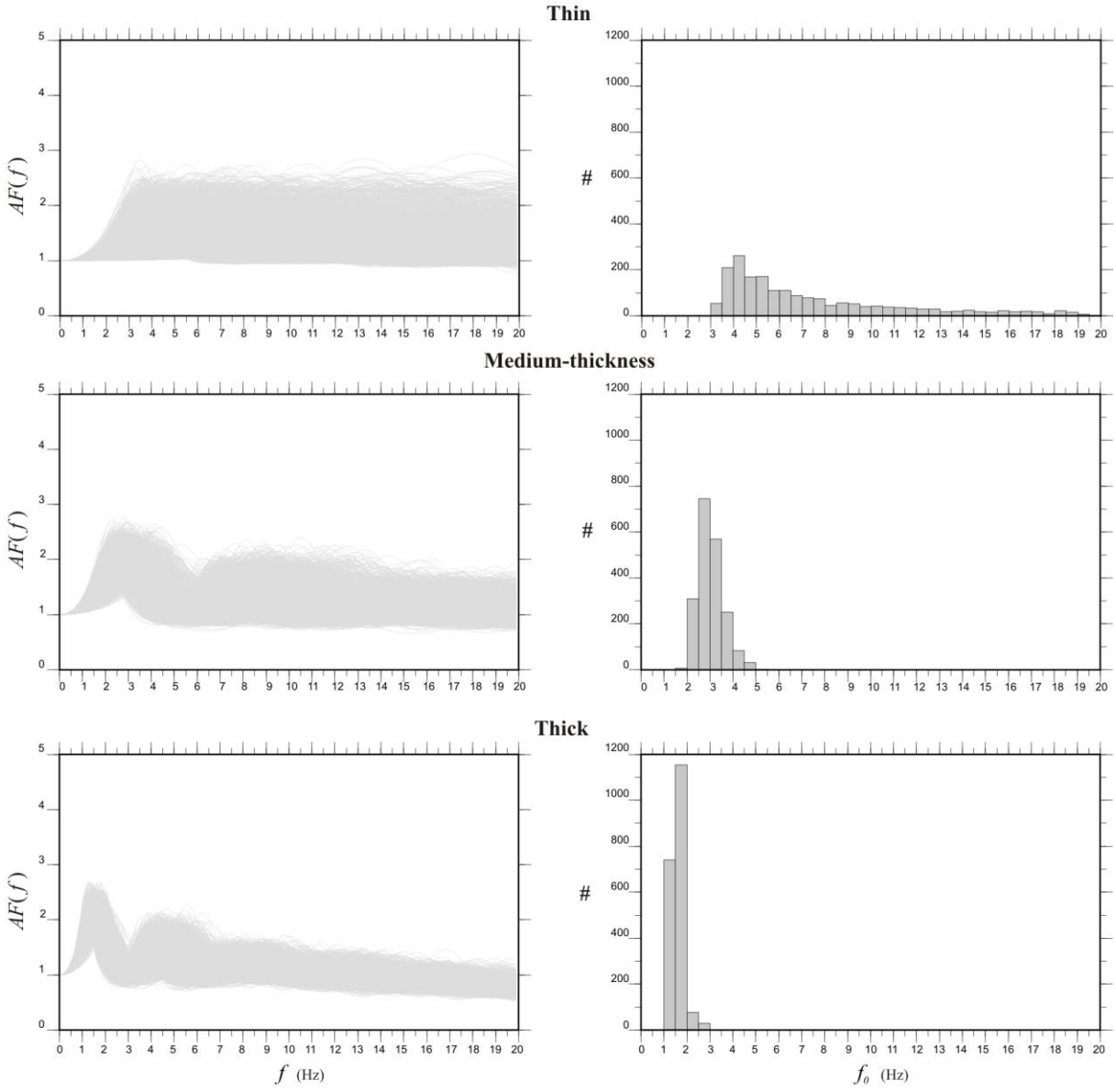

Figure 10

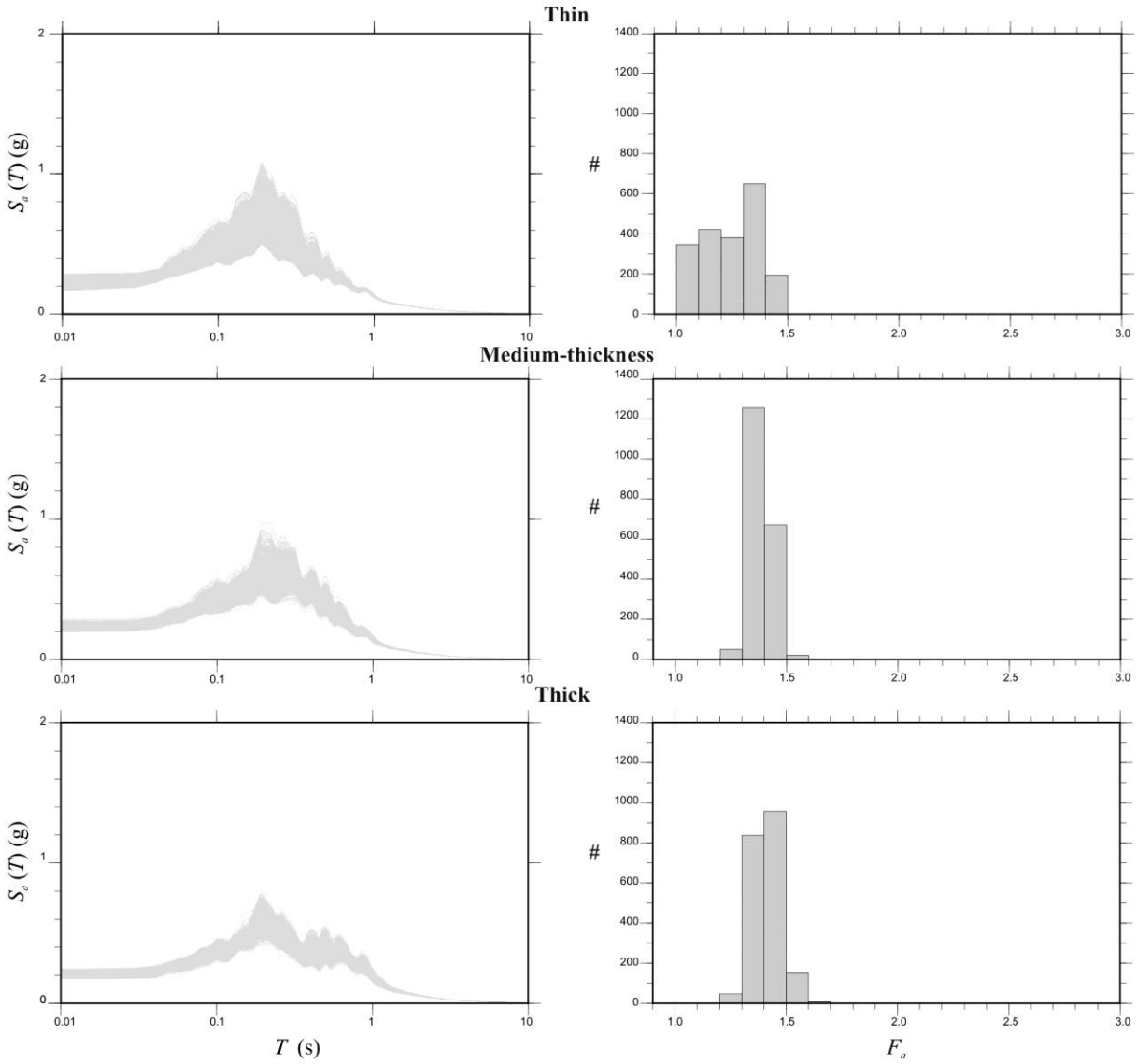

Figure 11

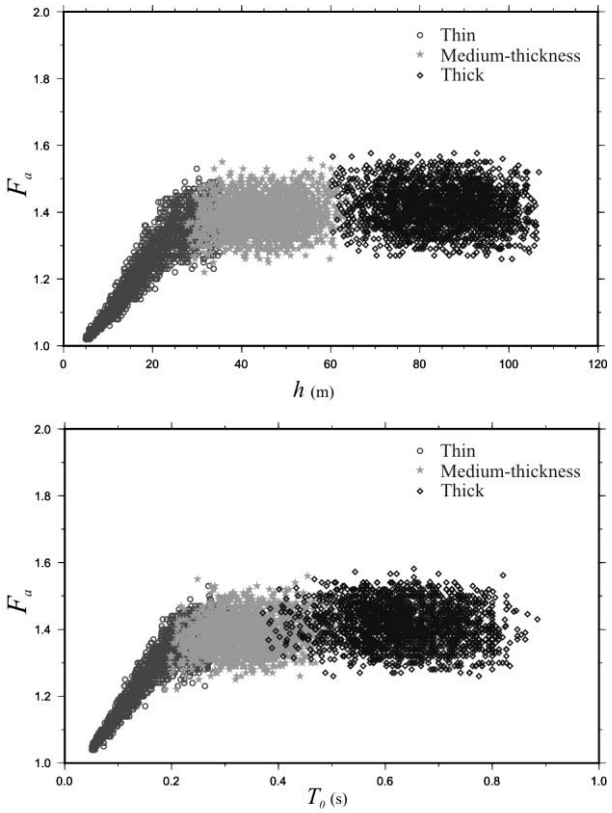
Thin
Medium-thickness
Thick
F_a
h (m)
Thin
Medium-thickness
Thick
F_a
T_0 (s)

Figure 12

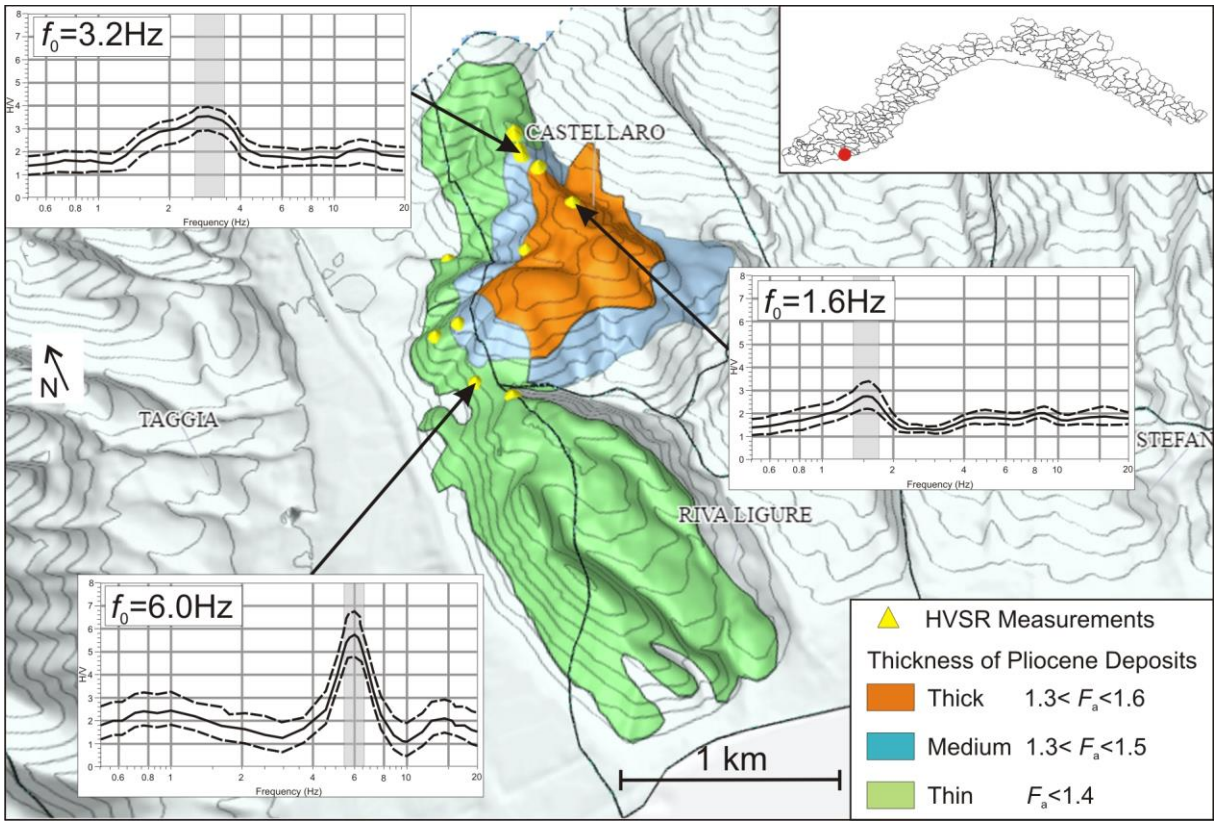
f_0=3.2Hz
f_0=1.6Hz
f_0=6.0Hz
Frequency (Hz)
HVSR
CASTELLARO
TAGGIA
RIVA LIGURE
STEFAN
N
1 km
HVSR Measurements
Thickness of Pliocene Deposits
Thick 1.3< F_a<1.6
Medium 1.3< F_a<1.5
Thin F_a<1.4